

Searching for a source of difference in Gaussian graphical models

Vera Djordjilović¹ & Monica Chiogna²

¹ Department of Biostatistics, University of Oslo, Norway

² Department of Statistical Sciences, University of Bologna, Italy

Abstract

In this work, we look at a two-sample problem within the framework of Gaussian graphical models. When the global hypothesis of equality of two distributions is rejected, the interest is usually in localizing the source of difference. Motivated by the idea that diseases can be seen as system perturbations, and by the need to distinguish between the origin of perturbation and components affected by the perturbation, we introduce the concept of a *minimal seed set*, and its graphical counterpart a *graphical seed set*. They intuitively consist of variables driving the difference between the two conditions. We propose a simple testing procedure, linear in the number of nodes, to estimate the graphical seed set from data, and study its finite sample behavior with a stimulation study. We illustrate our approach in the context of gene set analysis by means of a publicly available gene expression dataset.

Keywords: Gaussian graphical models, Decomposition, Two sample problem, Gene set analysis

1 Introduction

1.1 Two-sample problems in high dimensions: marginal vs. conditional approach

Let $X_V^{(1)}$ and $X_V^{(2)}$ denote two p -dimensional normal random vectors, indexed by the same variable set V , whose distributions we would like to compare. The first step is typically to test the global hypothesis of equality of the two distributions, but if that hypothesis is rejected, we would usually like to go a step further and localize the source of difference. When components within vectors are either assumed to be jointly independent, or little is known about their structure of dependence, a common approach, especially if p is large, is to focus on the p univariate marginal distributions.

Marginally speaking, a variable is considered a source of difference, and therefore relevant for the problem at hand, if its marginal distribution is different in the two conditions. If $\mathcal{L}(X)$ denotes the distribution of X , then the (index) set of the relevant variables is taken to be

$$R = \{v \in V : \mathcal{L}(X_v^{(1)}) \neq \mathcal{L}(X_v^{(2)})\}.$$

Whether a variable belongs to R depends solely on its marginal distribution.

Although this makes the marginal approach simple and computationally feasible, it often fails to answer the question of interest. For example, when the source of difference lies in the interactions between variables, the marginal approach will be unable to identify it. In these situations, and, more generally whenever we believe that the interplay between the variables plays an important role, it is reasonable to adopt the so-called conditional approach. The conditional approach takes into account the entire p -dimensional joint distribution, and flags a variable relevant only if the difference in its marginal distribution cannot be explained by the remaining variables. More precisely, the set of conditionally relevant variables D is:

$$D = \left\{v \in V : \mathcal{L}\left(X_v^{(1)} \mid X_{V \setminus \{v\}}^{(1)} = y\right) \neq \mathcal{L}\left(X_v^{(2)} \mid X_{V \setminus \{v\}}^{(2)} = y\right), y \in \mathbb{R}^{p-1}\right\}. \quad (1)$$

Since we assume $X^{(1)}$ and $X^{(2)}$ to be Gaussian, the equality of $\mathcal{L}\left(X_v^{(1)} \mid X_{V \setminus \{v\}}^{(1)} = y\right)$ and $\mathcal{L}\left(X_v^{(2)} \mid X_{V \setminus \{v\}}^{(2)} = y\right)$ for a single $y \in \mathbb{R}^{p-1}$ implies equality for all $y \in \mathbb{R}^{p-1}$. To identify D , one can thus compare p pairs of conditional distributions from (1). However, when p is large, the problem of testing equality of conditional distributions becomes extremely challenging, and represents an open area of research, see for instance Zhu and Bradic (2016) and references therein.

1.2 Our contribution: two sample problem in the Gaussian graphical modelling framework

We look at the problem of identifying D within the framework of Gaussian graphical models. To this aim, we introduce the assumption that the distributions of $X^{(1)}$ and $X^{(2)}$ obey the same Gaussian graphical law

$$M(G) = \{Y \sim \mathcal{N}(\mu, \Sigma), K = \Sigma^{-1} \in S^+(G)\},$$

where G is a known undirected (decomposable) graph and $S^+(G)$ is the set of positive definite matrices with null elements corresponding to the missing edges of G . In what follows, to facilitate the presentation of the work, we will refer to the set D as the *seed set*, and define it in a slightly different, though equivalent way in Section 2.1.

We translate the problem of identifying the seed set into a problem of testing equality of lower dimensional conditional distributions induced by the structure of G . To this aim, we rely on test statistics that exploit factorizations of the joint probability

distribution, and are functions of the quantities pertaining to the lower dimensional multivariate marginal distributions. The key advantage is that inference on marginal distributions is significantly less challenging than inference on conditional distributions. Beside the computational gain, we argue that the proposed approach addresses the issue of exploiting information on the structure of dependence in an efficient and elegant way. However, the stated advantages come at a cost: sometimes, the graphical structure is such that we are unable to identify D directly, but only its superset D_G , that we call the *graphical seed set* (see Definition 2). Relation between the two sets, that depends both on D and G , is studied in Section 3.

1.3 When can our approach be useful?

Our approach makes two key assumptions:

- (1.) information on the dependence structure, reflected in G , is available from previous studies or subject matter considerations;
- (2.) the underlying network G is sparse, i.e. the largest fully connected component (clique) is relatively small compared to the sizes of the two random samples from $X_V^{(1)}$ and $X_V^{(2)}$.

Although these assumptions are not always appropriate, we argue that there are important applications in which they are reasonable. One example is given by various biological networks, see Section 7.

1.4 The motivation and related work

The present work has been primarily motivated by the need to compare gene regulatory networks across two conditions. Since Gaussian graphical models have been used extensively as models for gene networks, this problem has led to numerous methodological contributions in the area. Most proposed approaches focus on inferring the graphical structure, either of the differential network (Zhao et al., 2014; Xia et al., 2015), or of the individual networks (Danaher et al., 2014; Mitra et al., 2016). Our approach is different in that, the structure, assumed to be known beforehand, is not the quantity of interest. Instead, the information provided by the structure is exploited in order to make inference on our quantity of interest: the set D .

1.5 The outline of the paper

In Section 2, we formally define the seed set and study its connection to different problems encountered in the high dimensional settings. In Section 3, we turn our attention to the Gaussian graphical modelling framework, and define the graphical seed set. In Section 4, we state the theoretical result regarding the decomposition of the global hypothesis of equality, that represents the main building block of our approach.

In Section 5, we propose the graphical seed set estimator and study its asymptotic and finite sample behavior from a theoretical point of view. In Section 6, we illustrate its finite sample performance with a simulation study, and finally, in Section 7, we give a biological validation of our approach. Section 8 concludes the paper and offers some potential directions for future research. Basic notions regarding graphs and graphical models are given in Appendix A, while proofs and technical details are reported in Appendix B.

2 The seed set

2.1 Definition

We start by introducing the seed set, and then provide its possible interpretations in different contexts.

Definition 1 (Seed set). *Let $X_V^{(1)}$ and $X_V^{(2)}$ be two normal random vectors indexed by the set V . We call the set $D \subseteq V$ the seed set, if the conditional distributions $X_{\bar{D}}^{(1)} | X_D^{(1)}$ and $X_{\bar{D}}^{(2)} | X_D^{(2)}$ coincide, where $\bar{D} = V \setminus D$. Furthermore, we say that D is a minimal seed set, if no proper subset of it is itself a seed set.*

Remarks.

- In case of regular normal distributions, a minimal seed set always exists and is unique.
- The minimal seed set is the smallest subset of variables that explains the difference between the two conditions: after conditioning on it, the distributions of the remaining variables are identical.
- If distributions of $X^{(1)}$ and $X^{(2)}$ are identical, the minimal seed set is an empty set.
- If D is a seed set, then any $D' \supset D$ is also a seed set.
- The number of potential seed sets for a pair of p -dimensional distributions is 2^p .

The above given definition is expressed in purely mathematical terms, with no reference to any particular context or problem. In the following sections, we re-interpret the seed set definition in relation to some common issues in modelling and inference.

2.2 Variable selection

In the context of classification or regression, variable selection is intended to select the best subset of predictors. Reasons for performing variable selection include: (i) improving statistical accuracy and addressing the curse-of-dimensionality; (ii) reducing the computational complexity; and finally (iii) improving model interpretability.

Koller and Sahami (1996) first showed that the Markov blanket of a given target variable is the theoretically optimal set of features to predict its value. For a given set of variables X_V , the Markov blanket (Pearl, 1988, Section 3.2.1) of a variable X_v , $v \in V$, is given by the smallest set $D \subset V$, such that X_v is conditionally independent of $X_{V \setminus \{D \cup \{v\}\}}$ given X_D . In other words, X_D is “shielding” X_v from the remaining variables.

Following our definition, the seed set is the Markov blanket of the class attribute representing the two populations under study. More precisely, let C represent a binary trait of interest, such as healthy/diseased, and let category labels be 1 and 2, instead of the customary 0 and 1. Consider the problem of modelling C as a function of a p -dimensional random vector of covariates X , indexed by V . Assuming that the distribution of X given $C = j$ is normal with parameters $\mu^{(j)}$ and $\Sigma^{(j)}$, $j = 1, 2$, we have $P(C = 1 \mid X = x) = 1 / \{1 + g(x)\}$, where

$$g(x) = \exp \left[c + \frac{1}{2} x^\top \{K^{(1)} - K^{(2)}\} x + x^\top \{K^{(1)} \mu^{(1)} - K^{(2)} \mu^{(2)}\} \right],$$

where $c \in \mathbb{R}$ is a constant, and $K^{(j)} = (\Sigma^{(j)})^{-1}$, $j = 1, 2$. The minimal seed set D is then the smallest subset of V such that g depends on X only through X_D . In other words, conditionally on X_D , the trait C is independent of $X_{V \setminus D}$, and X_D represents the Markov blanket of C .

Recently, in the context of high-dimensional variable selection, Candès et al. (2018) proposed a procedure for identifying the Markov blanket of a response while controlling false discovery rate. Their approach is general as no assumption is made on the conditional distribution of a response given covariates, but the joint distribution of covariates $\mathcal{L}(X)$ is assumed fully known. Our approach addresses the same problem when the response is binary, but under different assumptions. We assume that the conditional law $\mathcal{L}(X \mid C = j)$ is normal, with unknown parameters $\mu^{(j)}$ and $\Sigma^{(j)}$, $j = 1, 2$. From Section 3, we will further assume that there is a known undirected graph $G = (V, E)$, where $E \subseteq V \times V$ is a set of edges, such that $K^{(j)}$ have zeroes corresponding to the missing edges of G . This assumption ensures that the laws $\mathcal{L}(X \mid C = j)$, although potentially different, are Markov with respect to the same graph.

2.3 Discriminative dimension reduction

Two apparently distinct problems, particularly cogent in high dimensional regimes, often arise in the context of discriminant analysis. From one side, a lower dimensional feature vector is searched for such that it keeps only classification-relevant information of a raw input vector X about class labels C . A critical question of discriminative dimension reduction methods is how to measure the effectiveness of the lower dimensional feature vector in terms of preserving this classification-relevant information. On the other side, while several explanatory variables exist for discrimination, none might be sufficiently sensitive and specific on its own, so that a combination of variables is searched for having discriminating performances optimal in some sense.

If we interpret the two-sample problem as a classification problem, it emerges that X_D is the so-called smallest dimension reduction subspace (Cook and Yin, 2001), as $P(C | X_D) = P(C | X)$. Moreover, X_D allows to easily derive the classification rule, optimal in the sense that its receiver operating characteristic curve is maximized at every point. Indeed, a key result from decision theory, the Neyman-Pearson lemma, states that, for any fixed false positive rate, the discriminant rule with the highest true positive rate based on X , among all possible rules based on X , is the likelihood ratio rule. As

$$LR(X) = \frac{P(X | C = 1)}{P(X | C = 2)} = \frac{P(X_D | C = 1)}{P(X_D | C = 2)},$$

the Neyman-Pearson result states that the combination of variables resulting from exploiting the likelihood ratio function for X_D , and rules based on its exceeding a threshold, achieve the highest true positive rate among all rules based on X .

2.4 Reverse engineering of interventions

In statistics and machine learning, external interventions are usually debated in the context of causal discovery. Causal discovery or reverse engineering of causal structures (see Heinze-Deml et al., 2018, for a recent review) aims to infer the underlying causal structure on the basis of observational and/or experimental data. Since, in general, observational data are unable to distinguish between statistical associations and causal relations, a problem of interest is to find the optimal set of interventions so that the ability to uncover causal relations is maximized, while the experimental cost and complexity are minimized (He and Geng, 2008). The solution to this problem is far from being simple.

On a different side, various applications motivate a different kind of reverse engineering. In these instances, experimental data come from uncontrolled or partially controlled interventions with unknown targets (Eaton and Murphy, 2007). As an example, consider experiments in molecular biology in which it is not fully known how introducing different chemicals affects the system under study. In particular, a chemical can perturb a single variable, which can in turn affect multiple variables under study. A question of interest is then: given that an external intervention has occurred – chemical has been introduced – which of the variables under study – genes, proteins or metabolites – have been directly targeted? Problems of this kind characterize an area of interest that we call reverse engineering of interventions.

If we interpret the two distributions from the definition of the seed set as describing (a) the control condition of a system, and (b) the condition of the same system after an unknown intervention has taken place, then the minimal seed set consists of targets of that intervention. Hence, within this framework, estimating the seed set can be seen as inferring the target(s) of an unknown intervention based on the samples from a control and post-intervention distribution.

3 The graphical seed set

The minimal seed set is defined on the basis of comparing two p -dimensional joint distributions. The challenge of inferring the minimal seed set from data thus grows rapidly with increasing p . However, when comparing two normal distributions Markov with respect to the same graph, significant relief is possible. From here on, we turn our attention to Gaussian graphical models and the identification of the seed set that takes advantage of the graphical structure.

Definition 2 (Graphical seed set). *Let D be a minimal seed set for $X_V^{(1)}$ and $X_V^{(2)}$, two Gaussian graphical distributions Markov with respect to a decomposable, undirected graph $G = (V, E)$, where V is a set of nodes and E is a set of edges. Let $\mathcal{S} = \{S : S \text{ is a separator in } G\}$ be a collection of separators in G . Then we call the set*

$$D_G = \{v \in V \mid \nexists S \in \mathcal{S}, \text{ s.t. } v \notin S \text{ and } S \text{ separates } v \text{ from } D \text{ in } G\} \quad (2)$$

a graphical seed set.

Remarks.

- Note that S separates v from D when all paths between v and any element of D pass through some element of S . We allow for non-empty intersection between S and D , as well as $S = D$.
- For $v \in D$, the condition (2) is trivially satisfied (v cannot be separated from D by any set), and therefore $D_G \supseteq D$.
- When the minimal seed set is a separator, we can set $S = D$ in (2), to obtain $D = D_G$. In general, D and D_G will coincide whenever D can be expressed as an intersection of two or more cliques. In other instances, D_G will be a seed set, but not a minimal one.

The graphical seed set D_G is thus the smallest set containing the seed set D that can be identified by means of set operations on cliques and separators of G .

Example. We use a small undirected graph G shown in Figure 1 to illustrate various possible relations between the minimal seed set and the graphical seed set. G consists of cliques $C_1 = \{1, 2, 3\}$ and $C_2 = \{3, 4, 5\}$ separated by $S = \{3\}$. In the left panel, the minimal seed set $D = \{3\}$ coincides with the separator S , and thus with the graphical seed set as well. In the middle panel, the minimal seed set is $D = \{1, 3\}$. Node 2 is not separated from D by any separator in G (in this case, neither S nor empty set). Nodes 4 and 5 are separated from D by S , since all paths from 4 and 5 to D pass through S . The graphical seed set is thus $D_G = \{1, 2, 3\}$. In the right panel, the minimal seed set is $D = \{1, 4\}$. None of the remaining nodes 2, 3 and 5 is separated from D by a separator in G , and so the graphical seed set is the entire set of nodes $D_G = \{1, 2, 3, 4, 5\}$. \square

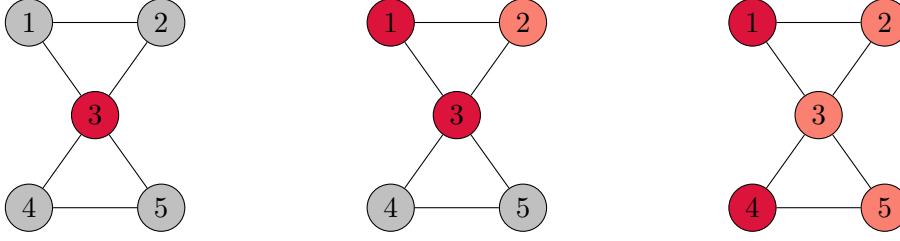


Figure 1: An example showing three minimal seed sets (dark red) and associated graphical seed sets (difference between the two in light red). On the left, the graphical seed set coincides with the minimal seed set; in the centre, the graphical seed set is larger than the minimal seed set; on the right, the graphical seed set is the entire set of nodes, although the minimal seed set consists of two nodes.

The above example illustrates that D_G might be larger than the set of interest, i.e. the minimal seed set D , and in some extreme cases might even cover the entire set of variables. However, in most situations it will allow us to zoom in on the set D , and the advantage is that if we focus on D_G , we can exploit the modularity of the graphical structure. Before we have a look at the proposed estimator in Section 5, we dedicate the next Section to the theoretical result underpinning our approach. In particular, we show how the global hypothesis of equality of two distributions belonging to the same Gaussian graphical model decomposes into a set of independent local hypotheses.

4 Decomposition of the global hypothesis of equality of two Gaussian graphical distributions

Let $G = (V, E)$ be a decomposable undirected graph on p vertices. Let C_1, \dots, C_k be a sequence of its cliques satisfying a running intersection property, and let S_2, \dots, S_k be an associated sequence of separators.

Theorem 1. *Let $X_1^{(1)}, \dots, X_{n_1}^{(1)}$ and $X_1^{(2)}, \dots, X_{n_2}^{(2)}$ be two random samples from $\mathbf{N}(\mu^{(1)}, \Sigma^{(1)})$ and $\mathbf{N}(\mu^{(2)}, \Sigma^{(2)})$, $\mu^{(l)} \in \mathbb{R}^p$, $(\Sigma^{(l)})^{-1} \in S^+(G)$, $l = 1, 2$, and consider the hypothesis of equality of distributions*

$$H : \mu^{(1)} = \mu^{(2)} \quad \text{and} \quad \Sigma^{(1)} = \Sigma^{(2)}. \quad (3)$$

Let $\lambda(V)$ denote the log likelihood ratio criterion for testing (3) and let $\lambda(A)$ denote the log likelihood ratio criterion for testing $H_A : \mu_A^{(1)} = \mu_A^{(2)}$ and $\Sigma_A^{(1)} = \Sigma_A^{(2)}$ for $A \subseteq V$. The following equality holds

$$\lambda(V) = \lambda(C_1) + \sum_{j=2}^k [\lambda(C_j) - \lambda(S_j)], \quad (4)$$

Moreover, the k terms on the right hand side of (4) are asymptotically independent under the null hypothesis.

It is worth noting that the terms in the summation on the right handside represent the likelihood ratio test statistic for the test of equality of conditional distributions $X_{C_j \setminus S_j} \mid X_{S_j}$, $j = 2, \dots, k$. This feature plays a crucial role when estimating D_G in Section 5.

5 Estimation

5.1 The graphical seed set estimator

We have seen above that, within the framework of Gaussian graphical models, the global hypothesis of equality can be decomposed according to a specified perfect ordering into a set of local independent hypotheses. By independent hypotheses, we mean that there are no logical relations between them, and that all combinations of true and false hypotheses are possible. However, the perfect ordering is not unique. In fact, there are multiple decompositions of the global hypothesis, each corresponding to a different factorization of the same distribution. It is this multiplicity that we exploit when estimating the graphical seed set.

For a given graph, the enumeration of all decompositions might resemble the problem of enumerating its junction trees (Thomas and Green, 2009), but a closer look reveals that it is a far simpler task. Given the uniqueness of the sequence of separators, it is not difficult to show that there is exactly one decomposition for each choice of the root clique – the clique labeled C_1 – leading to a total of k decompositions.

Before we show how these different decompositions relate to the graphical seed set in Proposition 2, we introduce some notation and restate the testing problem (3) in decision theory terms. Let Θ be the unrestricted parameter space of $(\mu^{(l)}, \Sigma^{(l)})$, $l = 1, 2$ where $(\Sigma^{(l)})^{-1} \in S^+(G)$, $l = 1, 2$; let Θ_0 denote the space restricted by H in (1), and let $\Theta_1 = \Theta \setminus \Theta_0$. We want to test $H : \theta \in \Theta_0$ against a general alternative $\theta \in \Theta_1$. Let the decision taken on H be denoted by d , where $d = 0$ means that the null hypothesis is not rejected and $d = 1$ means that the null hypothesis is rejected. A test ϕ is a mapping from the sample space to the set $\{0, 1\}$ (we rule out the trivial case that the test makes no decisions). Let d^* denote the correct decision (the truth) for the null hypothesis in (3). As seen in the previous Section, the null hypothesis can be decomposed into a set of independent local hypotheses, i.e., $H = \bigcap_{j=1}^k H_j$, and we denote by d_j^* the correct decision for H_j , $j = 1, \dots, k$, so that $d^* = (d_1^*, \dots, d_k^*)$. To identify the i -th decomposition, obtained when C_i is set as the root clique, we let $C_{i,1}, \dots, C_{i,k}$ denote a sequence of cliques satisfying the running intersection property. Let $S_{i,2}, \dots, S_{i,k}$ be an associated sequence of separators, and set $S_{i,1} = \emptyset$, $i = 1, \dots, k$. In this notation, $H_{i,j}$ will denote the j -th null hypothesis in decomposition i , $\phi_{i,j}$ the corresponding test, and $d_{i,j}^*$ the associated correct decision.

We now show the connection between the graphical seed set and the decompositions obtained from the graph G .

Proposition 1. *Let $d_i^* = (d_{i,1}^*, \dots, d_{i,k}^*)$ be the vector of correct decisions for the hypotheses $H_{i,j}$ of equality of distribution of $X_{C_{i,j} \setminus S_{i,j}} \mid X_{S_{i,j}}$ in the i -th decomposition. We then have*

$$D_G = \bigcap_{i=1}^k \bigcup_{\{j: d_{i,j}^*=1\}} C_{i,j}.$$

The above proposition gives an oracle procedure for recovering the graphical seed set from the knowledge of the two joint distributions. In practice, we need to rely on statistical tests. Let $\phi_i = (\phi_{i,1}, \dots, \phi_{i,k}) \in \{0, 1\}^k$ be a vector indicating the results of the statistical tests performed in the i -th decomposition, $i = 1, \dots, k$, with $\phi_{i,j} = 1$ when the hypothesis $H_{i,j}$ is rejected, and $\phi_{i,j} = 0$ otherwise. The following definition naturally follows.

Definition 3 (Graphical seed set estimator). *The random set \hat{D}_G , defined as*

$$\hat{D}_G = \bigcap_{i=1}^k \bigcup_{\{j: \phi_{i,j}=1\}} C_{i,j} \tag{5}$$

is an estimator of D_G .

Remark. As already stated, to estimate the minimal seed set from data one would, in general, compare pairs of p -dimensional conditional distributions, which becomes challenging with increasing p . In contrast, thanks to Theorem 1, estimating the graphical seed set requires computing at most $2k - 1$ test statistics in the smaller marginal models induced by cliques and separators.

5.2 Asymptotic behavior

Estimator \hat{D}_G is different from classical estimators in that its values depend on data through the results of sequences of tests. Properties of the estimator will ultimately depend on the properties of the tests which are used. A treatment of these properties in the limit of infinite data benefits from the introduction of a more general notion of consistency of tests, that we give in general terms as follows.

Definition 4. *A sequence of tests $\phi(n)$ for the hypothesis $H : \theta \in \Theta_0$ vs $H_1 : \theta \in \Theta_1$ is consistent if for each $\theta \in \Theta$ there exists a sequence of significance levels α_n s.t.*

$$(1) \text{ for each } \theta \in \Theta_0, \quad \lim_{n \rightarrow \infty} \mathbb{P}_\theta(\phi(n) = 1) = 0;$$

$$(2) \text{ for each } \theta \in \Theta_1, \quad \lim_{n \rightarrow \infty} \mathbb{P}_\theta(\phi(n) = 0) = 0.$$

In other words, a sequence of tests is consistent if, at least asymptotically, it reports a correct decision.

Let us now consider testing $H_{i,j}$ in the above given framework. Let $n = n_1 + n_2$ and assume that as $n \rightarrow \infty$, $n_l/n \rightarrow \gamma_l$ such that $0 < \gamma_l < 1$, $l = 1, 2$, and $\gamma_1 + \gamma_2 = 1$. Moreover, let the test statistic $\phi_{i,j}(n)$ be defined as

$$\phi_{i,j}(n) = \begin{cases} 0 & \lambda_{i,j;n} < q_n \\ 1 & \lambda_{i,j;n} > q_n \end{cases}$$

where $\lambda_{i,j;n}$ is the log likelihood ratio for $H_{i,j}$ and q_n a suitable sequence of quantiles. Standard results assure that, under the null hypothesis, the sequence $\lambda_{i,j;n}$ converges to a chi-square distribution with f degrees of freedom, where f is the difference between the dimensions of the unrestricted parameter space and the restricted parameter space implied by the hypothesis of equality of the distributions of $X_{C_{i,j} \setminus S_{i,j}} \mid X_{S_{i,j}}$ in the two groups. Then, the test that rejects the null hypothesis if $\lambda_{i,j;n}$ exceeds the upper α -quantile of the chi-square distribution is asymptotically of level α . We can state the following proposition.

Proposition 2. *In the framework stated above, for each $H_{i,j}$, there exists a sequence of significance levels α_n , s.t. the sequence of tests $\phi_{i,j}(n)$ is consistent.*

Theorem 2. *The estimator \hat{D}_G is a pointwise consistent estimator of D_G , i.e., $\mathbb{P}_{\theta \in \Theta}(\hat{D}_G = D_G) \rightarrow 1$.*

Proof. For a fixed i , we have that $\phi_i(n) = (\phi_{i,1}(n), \dots, \phi_{i,k}(n)) \rightarrow d_i^* = (d_{i,1}^*, \dots, d_{i,k}^*)$, since the inequality

$$\mathbb{P}_{\theta \in \Theta}(\phi_i(n) = d_i^*) \geq 1 - \sum_{j=1}^k \mathbb{P}_{\theta \in \Theta}(\phi_{i,j}(n) \neq d_{i,j}^*)$$

in conjunction with Proposition 2 implies $\mathbb{P}_{\theta \in \Theta}(\phi_i(n) = d_i^*) \rightarrow 1$. Convergence of \hat{D}_G to D_G follows straightforwardly. \square

5.3 Finite sample behavior

With finite samples, it is customary to assign a bound to the probability of incorrectly rejecting the null hypothesis by imposing conditions such as $\mathbb{P}_{\theta \in \Theta_0}(\phi_{i,j}(n) = 1) \leq \alpha$. Estimation of D_G requires performing a collection of $k + \sum_{i=1}^k \nu(C_i)$ tests, where $\nu(C_i)$ denotes the number of separators contained within the clique C_i . Finite sample behavior of \hat{D}_G thus hinges on the proper control of the multiplicity issue.

If we wish to control the inclusion of false positives in \hat{D}_G , the simplest approach is to control the familywise error rate (FWER) by applying the Bonferroni correction with a factor of $k + \sum_{i=1}^k \nu(C_i)$. However, the Bonferroni correction can be overly conservative in this situation since logical relations among subsets of hypotheses result

in a high positive dependence between the associated p -values. To address this issue, we employ the $\max T$ method of Westfall and Young (1993), which uses permutations to obtain the joint distribution of the p -values and, by accounting for the dependence among p -values, attenuates the conservativeness of the Bonferroni procedure. In our setting, the condition of subset pivotality is satisfied, and the Westfall and Young procedure controls the FWER in the strong sense.

When FWER for our collection of hypotheses is controlled at level α , the probability that \hat{D}_G contains a false positive, i.e. any $v \in V$, such that $v \notin D_G$, is at most α . In many applications, FWER control is considered too stringent and false discovery rate is considered instead. Although false discovery rate control can in our case be easily accomplished by standard methods, it is not clear how this control translates over to the properties of the graphical seed set estimator. For this reason, we restricted our attention to the FWER.

6 Simulation study

To study the finite sample behavior of \hat{D}_G , we considered a randomly generated graph, shown in Figure 2, consisting of 100 nodes grouped in 37 cliques (the largest clique containing 15 nodes). We set the parameters of the first, i.e. control, condition in the following way. The means of 100 variables were drawn randomly from a normal distribution centered at 0.5 (standard deviation 1). The matrix with all off-diagonal elements equal to 0.4 and all diagonal elements equal to 1 was modified so that its inverse has zeros corresponding to the missing edges of G .

For the second or post-intervention condition, we considered four different scenarios: one with no intervention, corresponding to the global null hypothesis, and three scenarios with interventions of different strength. Namely, the minimal seed set was set to $D = \{2, 5\}$, and in the post-intervention distribution the mean of the targeted variables was multiplied by a constant $\lambda \in \{1.1, 1.3, 1.7\}$ corresponding to a mild, moderate, and strong intervention, respectively. The variance of the two seed set variables was also manipulated: it was decreased by 50% in the post-intervention distribution. In this setting, the graphical seed set does not coincide with the minimal seed set since there is no separator in G that separates node 17 from D . We thus have $D_G = \{2, 5, 17\}$.

We assume that the considered intervention affects directly only the targeted variables, and leaves the mechanism underlying the conditional distribution of the remaining variables unaltered. As a consequence, the intervention indirectly affects the marginal distributions of $(X_1, \dots, X_{100})^\top$. This is illustrated by Figure 3 that compares the parameters associated to the first ten variables, i.e., X_1, \dots, X_{10} , before and after the intervention. Since all marginal univariate distributions differ between the two conditions, and so do all marginal clique distributions, univariate marginal approaches would correctly conclude that the condition under study affects all considered variables.

For each combination of the sample size $n = 50, 75, 100$, and the intervention scenario, we simulated 1000 pairs of samples. For each simulated pair, we computed

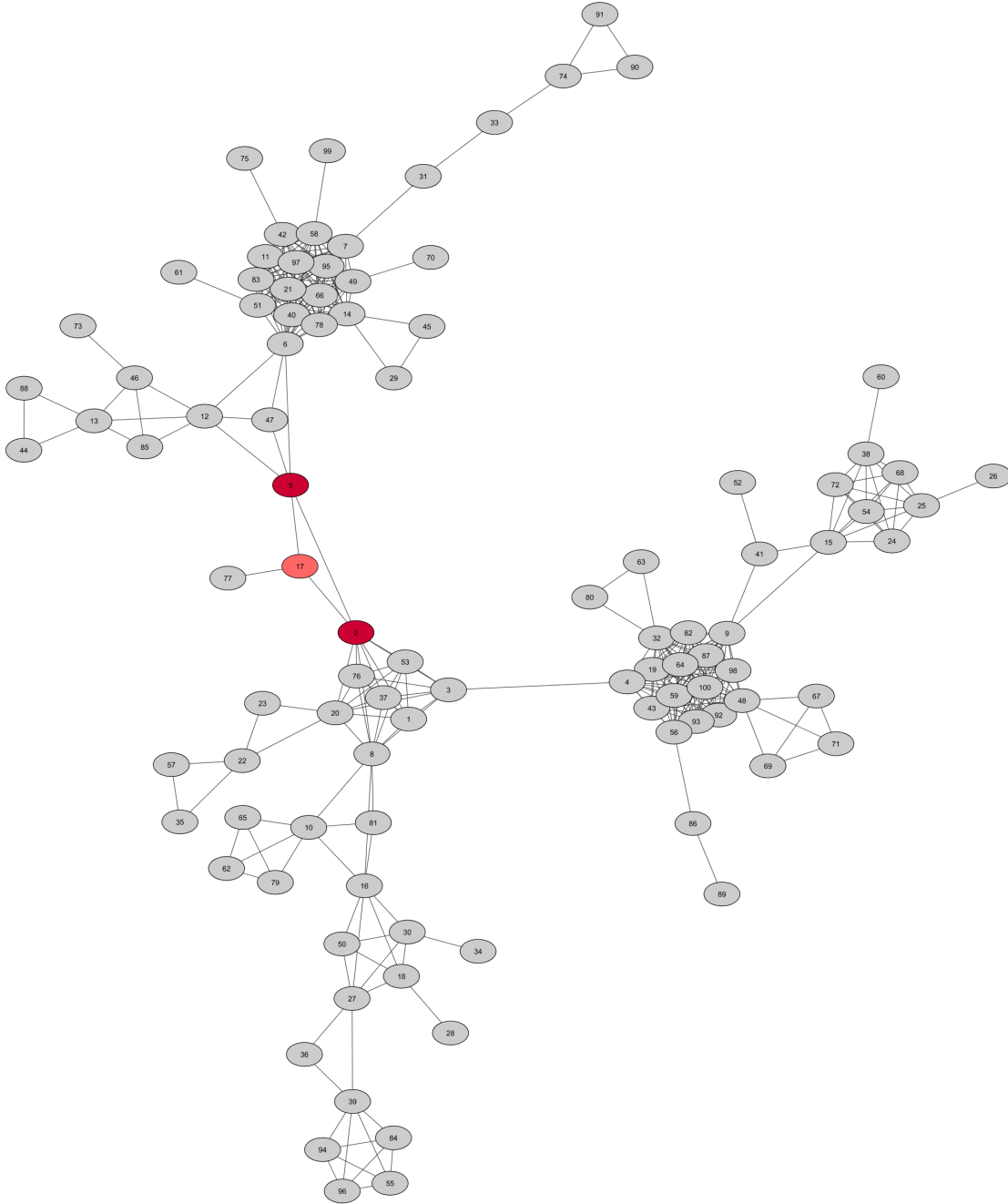


Figure 2: An undirected graph used in the simulation study. The minimal seed set is set to $D = \{2, 5\}$, shown in dark red, with the corresponding graphical seed set $D_G = \{2, 5, 17\}$.

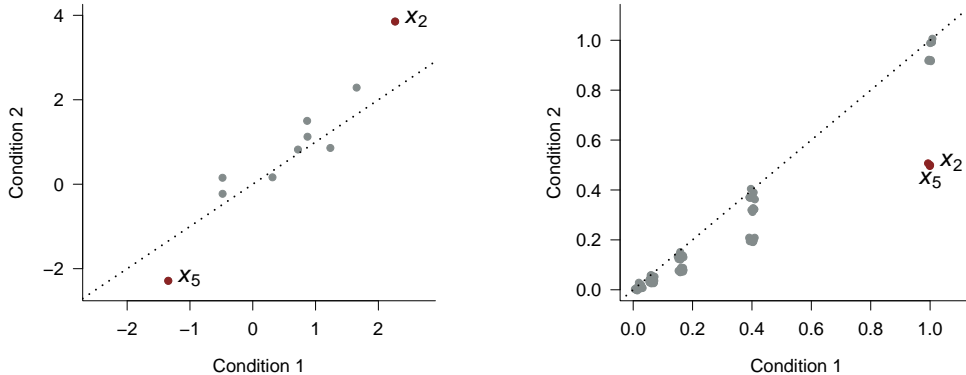


Figure 3: Simulation study: a comparison of the parameters in two conditions. On the left, the means of the first 10 variables, on the right, the associated elements of the covariance matrix. Means and variances of the seed set variables are highlighted in red. A dotted $y = x$ line is added for reference. A small noise is added to the plotted points on the right to avoid a complete overlap.

\hat{D}_G with the **SourceSet** R package, which implements the proposed approach (available from CRAN). The FWER was controlled at 5% by the step-down $\max T$ method (Westfall and Young, 1993) with $B = 500$ permutations. To evaluate the performance of our procedure, we looked at the number of times the estimated graphical seed set \hat{D}_G coincided with the true graphical seed set D_G . The results, shown in Table 1, regard the performance of our method only, since, to the best of our knowledge, there are no methods aiming to estimate a quantity similar to D_G .

We see that under the global null hypothesis the true seed set, $D_G = \emptyset$, is correctly identified approximately 98% of times, irrespective of the sample size. This is a consequence of the fact that by controlling the FWER at level 0.05, we are controlling at the same level the probability of including false positives in \hat{D}_G . This is true not only under the general null hypothesis (no intervention), but is valid in general, as can be seen from the estimated error rate, i.e. the average number of times the estimated graphical seed set contained a false positive, in other scenarios. On the other hand, not surprisingly, the performance under the alternative hypothesis depends on the strength of the intervention. When the intervention is strong, the power of the employed tests approaches 1 even for the smallest sample size ($n = 50$), and the seed set is identified correctly more than 95% of the times. When the intervention is weak, the power to detect it is low, and larger sample sizes are needed. This is evident from the mild intervention setting, where even for $n = 100$, the seed set was identified correctly only 16.9% of times. This is a consequence of our choice to control the inclusion of false positives: in case of low power, we are bound to obtain an estimate which is a subset

Table 1: Simulation study: the average number of times (out of 100) the graphical seed set was correctly identified in 12 different scenarios given by intervention strength and sample size. In parentheses, the average number of times the estimated graphical seed set contained a false positive.

| Intervention | Sample size | | | | | |
|--------------|-------------|-------|----------|-------|-----------|-------|
| | $n = 50$ | | $n = 75$ | | $n = 100$ | |
| None | 97.1 | (2.9) | 97.8 | (2.2) | 98.2 | (1.8) |
| Mild | 0.3 | (3.0) | 4.8 | (1.8) | 16.9 | (1.2) |
| Moderate | 26.3 | (2.9) | 80.4 | (2.1) | 95.6 | (1.9) |
| Strong | 95.3 | (4.0) | 97.2 | (2.8) | 97.5 | (2.5) |

of the true seed set.

7 Biological validation

7.1 Rationale

One of the most common aims in omics settings is the identification of genes that are differentially expressed between two or more biological conditions. To this aim, the most powerful multivariate methods use biological knowledge to define sets of functionally related genes (Goeman et al., 2004; Hummel et al., 2008; Tsai and Chen, 2009), which are then passed on to tools able to detect differential expression/co-expression of genes. Indeed, a large body of experimentally obtained knowledge regarding relations between genes is available, and usually stored in the form of diagrams called pathways (Kanehisa and Goto, 2000).

Coupling the biological knowledge stored in pathways with the potential of graphical models to efficiently represent structures of dependence, led Massa et al. (2010) to the formulation of a topological approach to gene set analysis, that transforms pathways into undirected graphs and models them as Gaussian graphical models. Within this pathway-centered framework, the problem of investigating differential expression/co-expression between two conditions is phrased as testing of equality of the mean/variance parameters of the distribution of two graphical models with the same graphical structure, the one representing the pathway.

Once the hypothesis of distribution equality is rejected, a biological explanation for the dysregulation is usually searched for. Translating detected dysregulations into claims about their origin is a challenging task. Chromosomal rearrangements offer a possible explanation. Chromosome rearrangements initiate various alterations of the regulation of gene expression through a variety of different mechanisms. For this reason, when comparing populations with and without a given gene rearrangement, sound

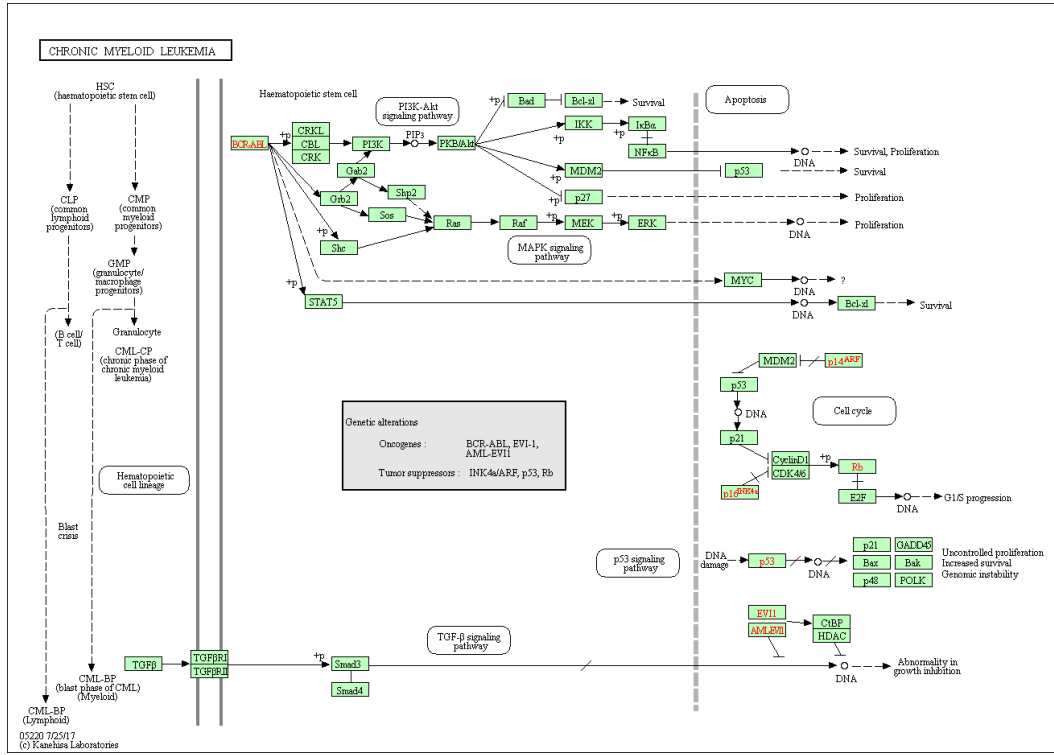


Figure 4: Chronic myeloid leukemia pathway from KEGG.

inferential tools usually flag most pathways including genes with the rearrangement as statistically different. What we should expect from tools calibrated to detect the source of dysregulation is that they go as close as possible to the rearranged genes. This is the reason why we consider known chromosomal rearrangements ideal case studies to explore the power of our procedure on real, complex and noisy data.

7.2 BCR/ABL fusion gene

As an example, consider the BCR/ABL fusion gene, formed by rearrangement of the breakpoint cluster region (BCR) on chromosome 22 with the c-ABL proto-oncogene on chromosome 9. This rearrangement causes production of an abnormal tyrosine kinase molecule with increased activity, postulated to be responsible for the development of leukemia and is present in all chronic myelogenous leukemia patients. It is also identified in some cases of acute lymphocytic leukemia (ALL), in which it is associated with poor prognosis.

Martini et al. (2013) consider a well-known dataset (Chiaretti et al., 2005) available from an R package ALL (Li, 2009), also analyzed in Dudoit and van der Laan (2008); Chen and Qin (2010); Li et al. (2012). Data refer to gene expression signatures of two groups of ALL patients: a first group of 37 subjects with BCR/ABL gene rearrangement, and a second group of 41 subjects without the BCR/ABL gene rearrangement.

By applying the approach of Massa et al. (2010), almost all pathways containing BCR and/or ABL genes are found to be statistically different.

Nevertheless, identifying BCR/ABL as a driver of the observed dysregulation might be difficult. In the same paper, Martini et al. (2013) propose an empirical algorithm to extract from a dysregulated pathway the portion mostly affected by the dysregulation. With specific reference to the Chronic myeloid leukemia pathway shown in Figure 4, a pathway whose functioning is highly impacted by BCR and ABL genes, the algorithm arrives at identifying 23 genes as involved in the dysregulation. This certainly allows to zoom into the functioning of the system; still, the special role of ABL and BCR genes in driving the dysregulation is far from being recognized.

7.3 The seed set output on Chronic myeloid leukemia pathway

We focused our attention on genes participating in the Chronic myeloid leukemia pathway (Figure 4). In detail, to derive the underlying undirected graph, we used the R package `graphite` Sales et al. (2016), which transforms KEGG pathways into graph objects. We moralized and triangulated this graph to obtain a decomposable graph. For graph operations, we relied on the package `gRbase` (Dethlefsen and Højsgaard, 2005). The obtained graph consists of three connected components, and for illustration purposes, we restricted our attention to the largest connected component, consisting of 27 nodes and 16 cliques, shown in Figure 5 (colors can be ignored for now). The number associated to each node is a unique gene identifier from the Entrez Gene database at the National Center for Biotechnology Information Maglott et al. (2005). Note that nodes 25 and 613 represent, ABL and BCR genes, respectively.

The hypothesis, shown in (3), of equality of distributions in the two groups is rejected by the likelihood ratio test (p -value = 2.06×10^{-11}). This is, of course, expected, since the two groups are defined on the basis of differences in genes 25 and 613. To see whether these differences are propagated over to the other genes, we can perform a test of equality of conditional distributions of the remaining genes given the central two. The obtained p -value, 6.65×10^{-3} , suggests rejecting the hypothesis of equality. We therefore decomposed the graph into a succession of cliques, in order to estimate the underlying graphical seed set.

In this case, there are 16 cliques, and thus 16 decompositions of the global null hypothesis. Across different decompositions, there are 41 unique local hypotheses. We controlled the FWER at 5% level by the $\text{min}P$ method with $B = 1640$ permutations (the minimal number recommended by the `SourceSet` package). We have thus relied on permutation, rather than asymptotic p -values in this case. Obtained p -values are shown in Table 2, in which tests whose null hypothesis is rejected are highlighted (the threshold found by $\text{min}P$ method was 2.4×10^{-3}). The results of these tests are then combined according to (5), and the result is represented in Figure 5. Highlighted nodes (either gray or red) belong to cliques that result significantly different in two conditions, while the red nodes form the estimated graphical seed set $\hat{D}_G = \{25, 613, 6776\}$. These three genes, thus, explain the marked difference between the two groups, but their

Table 2: Chronic myeloid leukemia dataset: decomposition of a two sample testing problem. Tests for which the null hypothesis was rejected are highlighted.

| No. | Test | p -value | No. | Test | p -value |
|-----|----------------------------------|----------------------|-----|-----------------------------------|----------------------|
| 1 | 1398, 1399, 25, 613, 867, 9846 | 6.0×10^{-4} | 21 | 25, 613, 6777 | 6.0×10^{-4} |
| 2 | 5295, 8503 1398, 1399, 867, 9846 | 3.9×10^{-1} | 22 | 25, 25759, 613 | 6.0×10^{-4} |
| 3 | 2885 25, 613, 9846 | 9.5×10^{-1} | 23 | 25, 4609, 613 | 6.0×10^{-4} |
| 4 | 207 5295, 8503 | 9.2×10^{-2} | 24 | 1147, 207, 3551 | 5.7×10^{-1} |
| 5 | 6776 25, 613 | 2.4×10^{-3} | 25 | 5295, 8503 207 | 8.2×10^{-2} |
| 6 | 6777 25, 613 | 9.3×10^{-1} | 26 | 1398, 1399, 867, 9846 5295, 8503 | 9.3×10^{-1} |
| 7 | 25759 25, 613 | 8.4×10^{-1} | 27 | 25, 613 1398, 1399, 867, 9846 | 6.0×10^{-4} |
| 8 | 4609 25, 613 | 1.7×10^{-1} | 28 | 207, 4193 | 4.4×10^{-1} |
| 9 | 1147, 3551 207 | 6.2×10^{-1} | 29 | 207, 5295, 8503 | 8.4×10^{-2} |
| 10 | 4790, 4792 1147, 3551 | 1.3×10^{-2} | 30 | 1147, 3551, 4790, 4792 | 5.0×10^{-2} |
| 11 | 6654, 6655 2885 | 3.6×10^{-1} | 31 | 207 1147, 3551 | 4.4×10^{-1} |
| 12 | 3265, 3845, 4893 6654, 6655 | 9.8×10^{-1} | 32 | 3265, 3845, 4893, 6654, 6655 | 8.8×10^{-1} |
| 13 | 369 3265, 3845, 4893 | 5.6×10^{-1} | 33 | 2885 6654, 6655 | 9.6×10^{-1} |
| 14 | 5894 3265, 3845, 4893 | 5.1×10^{-1} | 34 | 25, 613, 9846 2885 | 6.0×10^{-4} |
| 15 | 4193 207 | 3.3×10^{-2} | 35 | 3265, 3845, 4893, 5894 | 6.5×10^{-3} |
| 16 | 7157 4193 | 1.4×10^{-1} | 36 | 6654, 6655 3265, 3845, 4893 | 9.2×10^{-1} |
| 17 | 25, 2885, 613, 9846 | 6.0×10^{-4} | 37 | 3265, 369, 3845, 4893 | 6.8×10^{-1} |
| 18 | 1398, 1399, 867 25, 613, 9846 | 4.8×10^{-1} | 38 | 4193, 7157 | 1.3×10^{-2} |
| 19 | 25, 613, 6776 | 6.0×10^{-4} | 39 | 207 4193 | 4.4×10^{-1} |
| 20 | 1398, 1399, 867, 9846 25, 613 | 3.6×10^{-1} | 40 | 1398, 1399, 5295, 8503, 867, 9846 | 8.0×10^{-1} |
| | | | 41 | 2885, 6654, 6655 | 5.4×10^{-1} |

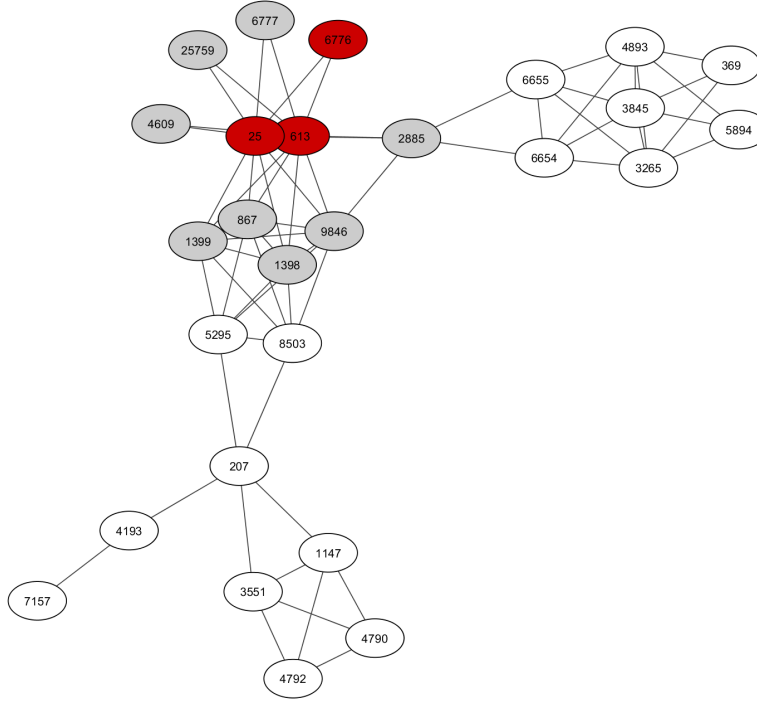


Figure 5: An undirected graph representing the Chronic myeloid leukemia pathway. Genes belonging to cliques for which the hypothesis of equality of distributions is rejected are highlighted. Genes belonging to the estimated graphical seed set are colored red.

effect does not seem to propagate towards other genes in the network (the majority of white nodes in Figure 5).

8 Discussion

Motivated by the differential analysis of gene networks, we have introduced the concept of the minimal seed set D , that intuitively consists of variables driving the difference between two conditions. In particular, we focus on comparing two multivariate normal distributions with the same graphical structure. Inferring D from data would in general require comparing pairs of high-dimensional conditional distributions, which is a highly challenging task. Our proposed approach shows that it is possible to replace this problem with the far simpler task of comparing a series of lower dimensional conditional distributions. Furthermore, no conditional distribution is estimated directly: test statistics are computed from quantities pertaining to the lower dimensional multivariate marginal distributions. This reformulation brings a significant computational relief: the analysis of the sizable graph considered in the simulation study, shown in Figure 2, takes around 4 seconds, with the most time consuming part being the permutation based $\max T$ method for controlling the FWER.

The price to be paid for this simplification is that we might not be able to identify the minimal seed set D , but only its superset and the graphical counterpart: the graphical seed set D_G . In some situations the graphical seed set might be too large to be useful. In others, when the size of the graphical seed set is sufficiently small compared to the available sample size, one can perform the second stage of testing to remove the redundant variables and arrive at the minimal seed set.

Our approach is based on the assumption that the graphical structure is known. Although there are important instances when this is the case, relaxing this assumption would bring a significant generalization of the method. Finding ways to combine learning of the graphical structure with the existing approach in an efficient way, while controlling the desired error rate, represents an open question that requires further research.

The proposed approach further relies on the assumptions that the underlying graphical structure is decomposable and shared between the two conditions. The assumption of decomposability does not seem to be particularly restrictive: if the original graph is not decomposable, it can be made into one by standard graphical manipulations such as moralization and triangularization. These operations usually lead to the addition of new edges. On the one hand, this can be seen as losing information represented by missing edges; on the other hand, these added edges embed the original graph in a denser graph, able to absorb possible uncertainties in the graphical structure, and also embrace potential local structural changes between two conditions, making the second assumption more plausible.

The basic building block of our method is the likelihood ratio statistic. Maximum likelihood estimates exist if and only if $\min\{n_1, n_2\} > \max_{i=1, \dots, k} |C_i|$, which implies that the method is applicable when the largest clique of the underlying graph is small enough with respect to the sizes of the two samples. Note that this also includes cases for which $\max\{n_1, n_2\} \ll p$, as long as cliques are sufficiently small. We are currently pursuing an extension in which the clique size is allowed to be larger than the sample size.

References

- Barndorff-Nielsen, O. (2014). *Information and exponential families in statistical theory*. John Wiley & Sons, New York.
- Candès, E., Y. Fan, L. Janson, and J. Lv (2018). Panning for gold: ‘model-X’ knockoffs for high dimensional controlled variable selection. *Journal of the Royal Statistical Society: Series B (Statistical Methodology)* 80(3), 551–577.
- Chen, S. X. and Y.-L. Qin (2010). A two-sample test for high-dimensional data with applications to gene-set testing. *The Annals of Statistics* 38(2), 808–835.
- Chiaretti, S., X. Li, R. Gentleman, A. Vitale, K. S. Wang, F. Mandelli, R. Foa,

- and J. Ritz (2005). Gene expression profiles of B-lineage adult acute lymphocytic leukemia reveal genetic patterns that identify lineage derivation and distinct mechanisms of transformation. *Clinical Cancer Research* 11(20), 7209–7219.
- Cook, R. D. and X. Yin (2001). Dimension reduction and visualization in discriminant analysis (with discussion). *Australian & New Zealand Journal of Statistics* 43(2), 147–199.
- Danaher, P., P. Wang, and D. M. Witten (2014). The joint graphical lasso for inverse covariance estimation across multiple classes. *Journal of the Royal Statistical Society: Series B (Statistical Methodology)* 76(2), 373–397.
- Dawid, A. and S. Lauritzen (1993). Hyper Markov laws in the statistical analysis of decomposable graphical models. *The Annals of Statistics* 21(3), 1272–1317.
- Dethlefsen, C. and S. Højsgaard (2005). A common platform for graphical models in R: The gRbase package. *Journal of Statistical Software* 14(17), 1–12.
- Dudoit, S. and M. J. van der Laan (2008). Multiple tests of association with biological annotation metadata. In *Multiple Testing Procedures with Applications to Genomics*, pp. 413–476. Springer.
- Eaton, D. and K. Murphy (2007). Exact Bayesian structure learning from uncertain interventions. In *Artificial Intelligence and Statistics*, pp. 107–114.
- Goeman, J. J., S. A. Van De Geer, F. De Kort, and H. C. Van Houwelingen (2004). A global test for groups of genes: testing association with a clinical outcome. *Bioinformatics* 20(1), 93–99.
- He, Y.-B. and Z. Geng (2008). Active learning of causal networks with intervention experiments and optimal designs. *Journal of Machine Learning Research* 9(–), 2523–2547.
- Heinze-Deml, C., M. H. Maathuis, and N. Meinshausen (2018). Causal structure learning. *Annual Review of Statistics and Its Application* 5(1), 371–391.
- Hummel, M., R. Meister, and U. Mansmann (2008). GlobalANCOVA: exploration and assessment of gene group effects. *Bioinformatics* 24(1), 78–85.
- Kanehisa, M. and S. Goto (2000). KEGG: Kyoto Encyclopedia of Genes and Genomes. *Nucleic Acids Research* 28(1), 27–30.
- Koller, D. and M. Sahami (1996). Toward optimal feature selection. In *Proceedings of the Thirteenth International Conference on International Conference on Machine Learning*, pp. 284–292.
- Lauritzen, S. L. (1996). *Graphical models*. Clarendon Press, Oxford.

- Li, J., S. X. Chen, et al. (2012). Two sample tests for high-dimensional covariance matrices. *The Annals of Statistics* 40(2), 908–940.
- Li, X. (2009). *ALL: A data package*. R package version 1.16.0.
- Maglott, D., J. Ostell, K. D. Pruitt, and T. Tatusova (2005). Entrez Gene: gene-centered information at NCBI. *Nucleic Acids Research* 33(suppl 1), D54–D58.
- Martini, P., G. Sales, M. S. Massa, M. Chiogna, and C. Romualdi (2013). Along signal paths: an empirical gene set approach exploiting pathway topology. *Nucleic Acids Research* 41(1), e19.
- Massa, M. S., M. Chiogna, and C. Romualdi (2010). Gene set analysis exploiting the topology of a pathway. *BMC Systems Biology* 4(1), 121.
- Mitra, R., P. Mller, and Y. Ji (2016, 03). Bayesian graphical models for differential pathways. *Bayesian Analysis* 11(1), 99–124.
- Pearl, J. (1988). *Probabilistic reasoning in intelligent systems: networks of plausible inference*. Morgan Kaufmann.
- Sales, G., E. Calura, and C. Romualdi (2016). *graphite: GRAPH Interaction from pathway Topological Environment*. R package version 1.20.1.
- Tan, W. (1977). On the distribution of quadratic forms in normal random variables. *Canadian Journal of Statistics* 5(2), 241–250.
- Thomas, A. and P. J. Green (2009). Enumerating the junction trees of a decomposable graph. *Journal of Computational and Graphical Statistics* 18(4), 930–940.
- Tsai, C.-A. and J. J. Chen (2009). Multivariate analysis of variance test for gene set analysis. *Bioinformatics* 25(7), 897–903.
- Westfall, P. H. and S. S. Young (1993). *Resampling-based multiple testing: Examples and methods for p-value adjustment*, Volume 279. John Wiley & Sons, New York.
- Xia, Y., T. Cai, and T. T. Cai (2015). Testing differential networks with applications to the detection of gene-gene interactions. *Biometrika* 102(2), 247–266.
- Zhao, S. D., T. T. Cai, and H. Li (2014). Direct estimation of differential networks. *Biometrika* 101(2), 253–268.
- Zhu, Y. and J. Bradic (2016). Two-sample testing in non-sparse high-dimensional linear models. *arXiv preprint arXiv:1610.04580*.

A Basics in graphical models

Here, we briefly review key notions regarding Gaussian graphical models, relevant for our work. For a detailed exposition, see Lauritzen (1996).

Consider an undirected graph $G = (V, E)$ where V is a set of nodes and E is a set of edges. A subset of vertices A defines an induced subgraph $G_A = (A, E \cap A \times A)$. A subgraph is said to be complete if all pairs of its vertices are connected in G . A clique is a maximal complete subgraph, that is, it is not a subset of any other complete subgraph.

Two disjoint subsets $A, B \subset V$ are said to be *separated* by a subset S (disjoint from A and B) if all paths from A to B contain vertices from S .

A graph G is decomposable if and only if the set of cliques of G can be ordered so as to satisfy the *running intersection property*, that is, for every $i = 2, \dots, k$

$$\text{if } S_i = C_i \cap \bigcup_{j=1}^{i-1} C_j \text{ then } S_i \in C_l \text{ for some } l < i - 1.$$

Although this ordering is generally not unique, the structure of the graph G uniquely determines the set of cliques $\{C_1, \dots, C_k\}$ and the set of *separators* $\{S_2, \dots, S_k\}$. For ease of notation, it is often set $S_1 = \emptyset$, so that the set of separators becomes $\{S_1, \dots, S_k\}$.

For simplicity, we consider only graphs consisting of a single connected component, although most of the presented notions remain valid for more general graphs. We also restrict our attention to decomposable graphs, and this assumption is central to our approach. We assume throughout that cliques have been ordered in an order satisfying the running intersection property. Since, in the following, we deal with different partitions of the set of vertices, we note that such an ordering naturally leads to several *partitions* of V . Recall that (A, S, B) is said to be a partition of V if A, S and B are disjoint and $V = A \cup S \cup B$. Partitions of V that correspond to *decompositions* of the graph G are of particular interest. For a graph $G = (V, E)$, a partition (A, S, B) of V is a decomposition of G if A and B are separated by S in G , and S is complete.

Denote $p = |V|$ and let $X \sim \mathbf{N}(\mu, \Sigma)$ be a p -variate normal random vector indexed by vertices of G . If Σ is invertible and such that its inverse, $K = \Sigma^{-1}$, has zeroes corresponding to missing edges of G , we say that X is a Gaussian graphical model. Let $S^+(G)$ denote the set of all symmetric $p \times p$ positive definite matrices with zeros corresponding to the missing edges of G . Moreover, for $A \subset V$, let Σ_A denote the corresponding block submatrix of Σ . In Gaussian graphical models, decompositions of the graph G correspond to special properties of the induced statistical models and associated inference procedures, as we will review in what follows.

Consider first the parameter $\theta = (\mu, \Sigma)$ of the model. If (A, S, B) is a decomposition of G , then X can be partitioned as (X_A, X_S, X_B) , where $X_A \perp\!\!\!\perp X_B \mid X_S$. Here, the conditional laws $\mathcal{L}(X_B \mid X_A, X_S)$ and $\mathcal{L}(X_B \mid X_S)$ coincide and are equal to

$$X_B \mid X_S \sim \mathbf{N} \left[\mu_B + \Sigma_{BS} \Sigma_S^{-1} (X_S - \mu_S), (K_B)^{-1} \right],$$

where $K_B = (\Sigma_B - \Sigma_{BS}\Sigma_S^{-1}\Sigma_{SB})^{-1}$. Split μ into two components, $\mu = (\mu_{AUS}, \mu_B)$ and partition Σ correspondingly. Then, parameters $\theta_{AUS} = (\mu_{AUS}, \Sigma_{AUS})$ and

$$\theta_{B|S} = (\mu_B - \Sigma_{BS}\Sigma_S^{-1}\mu_S, \Sigma_{BS}\Sigma_S^{-1}, K_B^{-1}),$$

(i.e., parameters of the marginal law of (X_A, X_S) and of the conditional law of $X_B | X_S$) are variation independent (Barndorff-Nielsen, 2014, p.28). It is worth noting that, on exploiting the symmetry of A and B with respect to S , we can analogously say that conditional laws $\mathcal{L}(X_A | X_B, X_S)$ and $\mathcal{L}(X_A | X_S)$ coincide and are equal to

$$X_A | X_S \sim \mathbf{N}[\mu_A + \Sigma_{AS}\Sigma_S^{-1}(X_S - \mu_S), (K_A)^{-1}],$$

where $K_A = (\Sigma_A - \Sigma_{AS}\Sigma_S^{-1}\Sigma_{SA})^{-1}$. Accordingly, parameters θ_{BUS} and $\theta_{A|S}$ are variation independent.

Consider now a random sample X_1, \dots, X_n from the same model and maximum likelihood estimation of θ . To estimate θ , we go through the estimation of θ_{AUS} and $\theta_{B|S}$. It is known that, beside being variation independent, these parameters are also L-independent since the likelihood function is of the product form: $L(\theta_{AUS}, \theta_{B|S}) = L(\theta_{AUS})L(\theta_{B|S})$, causing the covariance between their maximum likelihood estimators to vanish asymptotically. Therefore, $\hat{\theta}_{AUS}$ and $\hat{\theta}_{B|S}$ are asymptotically independent. Note that although this independence is reminiscent of the strong hyper Markov property, it holds only asymptotically, since the distribution of the maximum likelihood estimator is not strong hyper Markov unless Σ is diagonal (Dawid and Lauritzen, 1993). However, the sampling distribution of $\hat{\theta}$ defines a *weak hyper Markov law* on the parameter space (Dawid and Lauritzen, 1993). A weak hyper Markov property ensures that separations in the graph, reflected in the distribution of the original variables, are also reflected in the distribution of the maximum likelihood estimator. More precisely, it trivially holds

$$\hat{\mu}_{AUS} \perp\!\!\!\perp \hat{\mu}_{BUS} | \hat{\mu}_S,$$

and, more importantly,

$$\hat{\Sigma}_{AUS} \perp\!\!\!\perp \hat{\Sigma}_{BUS} | \hat{\Sigma}_S.$$

B Technical details and proofs

Proof of Theorem 1. Let $\lambda := \lambda(V)$. We recall the log likelihood ratio statistic for testing H

$$\lambda = \sum_{l=1}^2 n_l \log \frac{|\hat{\Sigma}|}{|\hat{\Sigma}^{(l)}|},$$

where $|\hat{\Sigma}|$ is determinant of the maximum likelihood estimate of Σ under H , $\hat{\Sigma}$, with

$$\hat{\Sigma} = \frac{1}{n_1 + n_2} \left[\sum_{i=1}^{n_1} (X_i^{(1)} - \bar{X})(X_i^{(1)} - \bar{X})^\top + \sum_{j=1}^{n_2} (X_j^{(2)} - \bar{X})(X_j^{(2)} - \bar{X})^\top \right],$$

where

$$\bar{X} = \frac{1}{n_1 + n_2} (n_1 \bar{X}^{(1)} + n_2 \bar{X}^{(2)}), \quad \bar{X}^{(l)} = \frac{1}{n_l} \sum_{i=1}^{n_l} X_i^{(l)}, \quad l = 1, 2,$$

and $\hat{\Sigma}^{(l)}$, $l = 1, 2$, are maximum likelihood estimates of $\Sigma^{(l)}$ under the general alternative, given by

$$\hat{\Sigma}^{(l)} = \frac{1}{n_l} \sum_{i=1}^{n_l} (X_i^{(l)} - \bar{X}^{(l)})(X_i^{(l)} - \bar{X}^{(l)})^\top, \quad l = 1, 2.$$

We recall that the asymptotic distribution of λ is chi square with $\text{card}(E) + 2p$ degrees of freedom, where $\text{card}(E)$ denotes the cardinality of E .

Since the determinant of every Ω for which $\Omega^{-1} \in S^+(G)$ can be decomposed with respect to the graph as $|\Omega| = \prod_{i=1}^k |\Omega_{C_i}| / \prod_{i=2}^k |\Omega_{S_i}|$, and therefore also the determinants of $\hat{\Sigma}$ and $\hat{\Sigma}^{(l)}$, $l = 1, 2$, the above equality can be equivalently written as

$$\lambda = \sum_{i=1}^k \lambda(C_i) - \sum_{i=2}^k \lambda(S_i),$$

from which the equality (4) follows.

The asymptotic independence of terms in the right-hand side of (4) can be seen as an immediate consequence of the hyper Markov property and the well known results regarding the maximum likelihood estimation in Gaussian graphical models. Let us first consider the case $k = 2$. Let C_1 , C_2 be the two cliques satisfying the running intersection property, S_2 be the associated separator, $A = C_1 \setminus S_2$, $S = S_2$ and $B = C_2 \setminus S_2$, so that (A, S, B) is a decomposition of G . It is easy to see that $H = H_1 \cap H_2$, where $H_1 : \theta_{A \cup S}^{(1)} = \theta_{A \cup S}^{(2)}$ and $H_2 : \theta_{B|S}^{(1)} = \theta_{B|S}^{(2)}$ concern variation independent parameters.

Exploiting the block structure of $\hat{\Sigma}_{B \cup S}$, we obtain $|\hat{\Sigma}_{B \cup S}| = |\hat{\Sigma}_S| |\hat{K}_B|$, and the equality (4) becomes

$$\lambda = \sum_{l=1}^2 n_l \log \frac{|\hat{\Sigma}_{A \cup S}|}{|\hat{\Sigma}_{A \cup S}^{(l)}|} + \sum_{l=1}^2 n_l \log \frac{|\hat{K}_B^{(l)}|}{|\hat{K}_B|}. \quad (6)$$

The first term on the right hand side, $\lambda(A \cup S)$, corresponds to the likelihood ratio test for the hypothesis of equality of marginal distributions induced by $A \cup S$, i.e., $H_{01} : \theta_{A \cup S}^{(1)} = \theta_{A \cup S}^{(2)}$. The second term, that we might informally denote as $\lambda(B | S)$, corresponds to the likelihood ratio test for the hypothesis of equality of conditional distributions induced by variables in B given the variables in S , i.e. $H_2 : \theta_{B|S}^{(1)} = \theta_{B|S}^{(2)}$. It is $\lambda(A \cup S) = \lambda(C_1)$ and $\lambda(B | S) = \lambda(C_2) - \lambda(S_2)$. Thanks to variation independence of the parameters in H_1 , H_2 and to their L-independence, this implies that $\lambda(A \cup S)$ and $\lambda(B | S)$ are asymptotically independent not only under H , but whenever one of the two hypotheses is true, i.e., under $H_1 \cup H_2$.

For $k > 2$, asymptotic independence for all pairs of subsequent components of (4) is proven analogously, which together with the characterizing property of the chi-square distribution (Tan, 1977) suffices to prove the joint asymptotic independence. \square

Proof of Proposition 1. Let $P = \bigcap_{i=1}^k \bigcup_{\{j: d_{i,j}^*=1\}} C_{i,j}$. Let D_G be the graphical seed set defined in (1). We want to show $P = D_G$. Let $v \notin D_G$. Then there is a $S \in \mathcal{S}$ separating v from D , and we choose S such that v and S are connected in G . Note that this is always possible for any $v \notin D_G$. Let C be a clique containing v and S . Then S must also be separating $C \setminus S$ and D . Using the properties of conditional independence and its connection to the graph separations, we have

$$\mathcal{L}(X_{C \setminus S} \mid X_S) = \mathcal{L}(X_{C \setminus S} \mid X_{D \cup S})$$

for any X_V Markov with respect to G . Since $D \cup S$ is a seed set, the distribution $\mathcal{L}(X_{C \setminus S} \mid X_S)$ is the same in two conditions and the associated null hypothesis is true leading to $d_{i,j}^* = 0$ for some $i, j = 1, \dots, k$. We therefore have $v \notin P$. All the steps relied on equivalence relations and thus $P = D_G$. \square

Proof of Proposition 2. Choose $\alpha_n = (1 - F_U(n^d))$, with $0 < d < 1/2$, $U \sim \chi_f^2$, and let $q_n = F_U^{-1}(\alpha_n)$. Under the null hypothesis, $\lambda_{i,j;n} \xrightarrow{d} \lambda$, with $\lambda \sim \chi_f^2$. Thanks to the Slutsky theorem, we can write

$$\mathbb{P}_{\theta \in \Theta_0}(\phi_{i,j}(n) = 1) = \mathbb{P}_{\theta \in \Theta_0} \left(\frac{\lambda_{i,j;n}}{n^d} > 1 \right) \longrightarrow 0.$$

Furthermore, for each $\theta_1 \in \Theta_1$, it is known that the log likelihood ratio test is degenerate with the order $O(\sqrt{n})$. With the choice of α_n above,

$$\mathbb{P}_{\theta_1}(\phi_{i,j}(n) = 0) = \mathbb{P}_{\theta_1} \left(\frac{\lambda_{i,j;n}}{n^d} < 1 \right) \longrightarrow 0, \quad \forall \theta_1 \in \Theta_1 \quad \square$$